RSC Advances

PAPER

View Article Online
View Journal | View Issue

Cite this: *RSC Adv.*, 2015, **5**, 2837

Naphthalimide-based fluorescent photoinduced electron transfer sensors for saccharides†

Shanshan Liu, Hongyan Bai, Qian Sun, Weibing Zhang and Junhong Qian*

Received 29th October 2014
Accepted 4th December 2014

DOI: 10.1039/c4ra13414a

www.rsc.org/advances

The design and synthesis of two novel fluorescent sensors based on the photoinduced electron transfer (PET) mechanism for the detection of saccharides in aqueous medium is described. These sensors are based on the 4-amino-1,8-naphthalimide fluorophore, which absorbs and emits at ~400 nm and ~530 nm, respectively. By incorporating a phenylboronic acid receptor at the 4-position through a piperazine linker, high sensitivity was achieved for the sensing of saccharides. Both probes showed pH-dependent fluorescence intensities, with pK_a values of 4.8 (**PET-S1**) and 4.4 (**PET-S2**), respectively. After binding with sugars, up to 50-fold and 5-fold fluorescence enhancements for **PET-S1** and **PET-S2** were observed at pH 7.4, which allows them to be used under physiological conditions. The switch-on responses of both probes toward saccharides demonstrating the suppression of PET from the amino group to the fluorophore. The probes showed high sensitivity towards D-fructose and D-sorbitol. Probe **PET-S1** was used to detect fructose in honey and beverages with good recovery.

Introduction

Blood glucose and fructose levels are closely related to some diseases such as hypoglycaemia, diabetes mellitus and hereditary fructose intolerance (HFI).[1] Therefore, quantitatively monitoring saccharides is of great importance in disease diagnosis and therapies. Fluorescence method has been proved to be a powerful technique in the detection of various metal ions, anions, proton, neutral organic molecules and gases due to its merits of sensitivity, selectivity, real time detection and fluorescent imaging.[2] Many fluorescent probes with phenylboronic acid as the receptor for saccharides have been synthesized over the past two decades.[3] Several strategies, such as photo-induced electron transfer (PET),[4] internal charge transfer (ICT),[5] fluorescence resonance energy transfer (FRET),[6] supramolecular assembles[7] and *etc.*,[8] were used to design fluorescent probes for sugars. Among these, PET mechanism has been wildly used to design fluorescent sensors for protons and metal ions.[9] However, construction of fluorescent sensors for neutral organic molecules is still a big challenge due to the small electronic changes upon guest binding. A PET-based fluorescent sensor usually consists of several distinct components: a fluorophore and a receptor linked by a spacer, which makes the design of various PET probes by molecular engineering be possible.[10]

A couple of PET sensors for saccharides have been reported.[4] However, those probes have the weaknesses of either small fluorescence intensity changes[4a] or relatively short emission maxima.[4b,c] As an ideal fluorescent probe, following requirements need to be considered: (1) absorbs and emits in visible region with large Stokes shift; (2) be water soluble and insensitive to the solvent polarity; (3) significant and selective fluorescence response toward analyte. In view of the stronger acidity of boronic acid upon polyol-binding and the tight and reversible binding between sugars and boronic acid, we intended to synthesize two PET proton sensors for the measurement of saccharides.

Naphthalimide is an often used fluorophore in the construction of chemosensors because of its absorption and emission being in visible region and its ease of modification.[11] Mohr *et al.*[4a] synthesized a phenylboronic acid derivative of 1,8-naphthalimide linked by a flexible aliphatic chain with an appended amino (**FR-530**). Nevertheless, only about 3-fold fluorescence enhancement was observed upon the addition of 100 mM of D-fructose. In the present work, we used more rigid and bulky piperazine instead of flexible aliphatic amine to strengthen the interaction between the boronic acid and the amino (**PET-S1** and **PET-S2**). Diglycolamine and *n*-butylamine were used to adjust the water solubility of the probes (Scheme 1). Sugar binding leads to an increase in the Lewis acidity of the boron atom, which therefore enhances the interaction between boronic acid moiety and the amino. Accordingly, significant fluorescence enhancements and relatively low detection limit could be expected.

Shanghai Key Laboratory of Functional Materials Chemistry, School of Chemistry and Molecular Engineering, East China University of Science and Technology, Shanghai, 200237, China. E-mail: junhongqian@ecust.edu.cn

† Electronic supplementary information (ESI) available: Experimental details of synthetic procedures, characterization and cell cultures, fluorescence titrations. See DOI: 10.1039/c4ra13414a

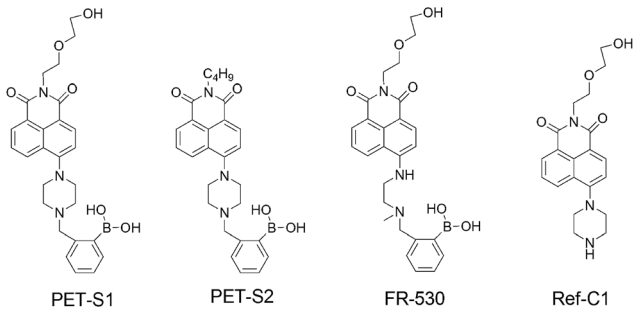

Scheme 1 The chemical structures of the compounds studied.

Results and discussion

Photophysical properties and water solubility of the two probes

Fig. 1a shows the absorption and emission spectra of **PET-S1** and **PET-S2**, from which it is observed that the absorption maxima of both probes are at about 400 nm, while the emission maxima are at 540 nm and 521 nm for **PET-S1** and **PET-S1**, respectively. The Stokes shifts for both compounds are large enough (~130 nm) to avoid the self-quenching. The fluorescence quantum yields of **PET-S1** ($\Phi_f = 0.007$, coumarin 153 was employed as the reference) and **PET-S2** ($\Phi_f = 0.065$) in PBS were relatively low, which indicates the potential application of both probes in the detection of saccharides under physiological conditions.

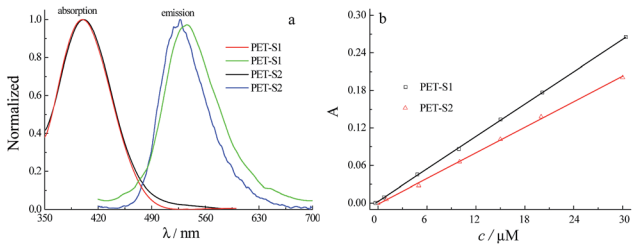

Fig. 1 Normalized absorption and emission spectra of probes **PET-S1** and **PET-S2** in phosphate buffer solution (a) and the linear correlation between the absorbance at 400 nm and the probe concentration (b). [**PET-S1**] = [**PET-S2**] = 10 μM, 50 mM PBS, pH 7.4, λ_{ex} = 400 nm.

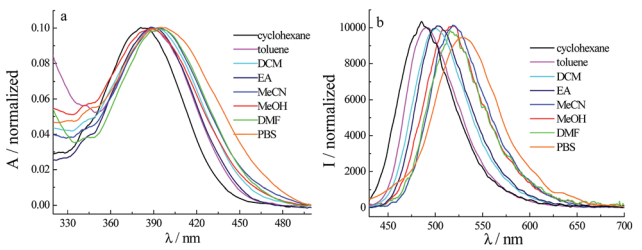

Fig. 2 Normalized absorption (a) and emission (b) spectra of **PET-S1** in various solvents.

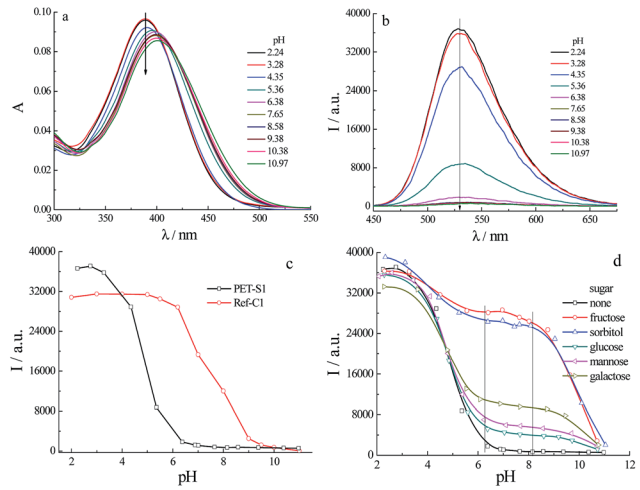

Fig. 3 pH effect on the absorption (a) and emission (b) spectra of **PET-S1**, and the fluorescence intensity pH profiles of **Ref-C1** (c) and **PET-S1** (d) in the absence and presence of sugars. [**PET-S1**] = 10 μM, [sugar] = 100 mM, 50 mM PBS, pH 7.4, λ_{ex} = 400 nm.

The water solubility of both probes in 50 mM phosphate buffer solution (PBS, pH 7.4) were determined by their concentration-dependent (0–30 μM) absorbance at 400 nm. Fig. 1b demonstrates that both probes were completely soluble in PBS at the concentration range of 0–30 μM (10 μM was used in this work). Therefore, the following experiments were conducted in pH 7.4 PBS/DMF (99 : 1). Fig. S1a† displays the concentration dependent fluorescence intensities (I_{530}) of both probes. Good linear relationship between I_{530} and [**PET-S1**] is observed over the range of 0–30 μM. However, a break point at about 5 μM is found in the I_{530}–[**PET-S2**] curve suggesting that self-aggregate forms at higher **PET-S2** concentrations.

Fig. S1b† illustrates the emission spectra of **PET-S1** and **PET-S2** in differently viscous media. It can be seen that with increasing viscosity both compounds become more fluorescence and the discrepancy between the two probes becomes smaller. These results reveal that both **PET-S1** and **PET-S2** are more rigid in viscous medium. The much higher quantum yield of **PET-S2** could be attributed to the aggregation at high concentrations, which leads to stronger N–B bonding and makes the PET process less effective (Fig. S1a and b†).

The photophysical properties of PET-S1 and PET-S2 in different solvents

Then, the polarity effect on the photophysical properties of both probes was studied by measuring their absorption and emission spectra in different solvents (Fig. 2 and S2†). Both compounds display distinctly solvatochromic UV-vis and fluorescence spectra: the absorption/emission of **PET-S1** shift from 385 nm/485 nm in cyclohexane to 400 nm/530 nm in PBS.

The fluorescence quantum yields of both compounds are relatively low in polar solvents such as DMF, MeOH and water (Table S1†); which is probably due to the photo-induced electron transfer from the piperazine to the fluorophore. In polar solvents, the orbit energy of HOMO becomes lower,

which facilitates the PET process. In addition, another decay pathway may be caused by the formation of hydrogen bonding in protic solvents.

pH responses of PET-S1 and PET-S2 with and without sugars

The pH profiles of both probes were investigated to better understand the sensing mechanism of the probes toward sugars. Fig. 3a shows that when pH changes from 2.24 to 10.97, the maximum absorbance as well as the fluorescence intensity of **PET-S1** decreases monotonously with slight red-shifts. The pK_a value of **PET-S1** calculated from the fluorescence intensity is ~4.8, which is lower than that of the reference compound without phenyl boronic acid (pK_a ≈ 7.5 for **Ref-C1**). The formation of B–N bond reduces the basicity of the amino group resulting in a lower pK_a value.[4d]

The presence of D-fructose (100 mM) evidently changes the fluorescence of **PET-S1** over a large pH range: the emission intensity decreases slightly as pH increasing from 2 to 6.3; it decreases remarkably as pH changing from 8.1 to 11.0; while it keeps almost the same in pH range of 6.3–8.1 (Fig. 3d). The fluorescence intensity pH profile of **PET-S1**-fructose suggests that there are two pK_a values, roughly at 4.1 and 9.7 as calculated from fluorescence measurements, for the saccharide complex. The previous one is probably from the fatty tertiary amine, while the latter could be ascribed to the phenyl boronic acid. Sorbitol induced similar fluorescence change of **PET-S1**, whereas other three sugars (glucose, mannose and galactose) triggered much smaller fluorescence changes. The pH profiles of **PET-S2** with and without sugars are similar to those of **PET-S1** (Fig. S3†). The stable and obvious fluorescence signal response for **PET-S1** toward the sugars in the pH range of 6.3 to 8.1 reveals the potential application of the probe for saccharide detection at physiological pH.

Compared to the reference (**Ref-C1**), the B–N bonding in **PET-S1** reduces the basicity of the fatty tertiary amine, as a result, the pK_a values of both probes are lower. At low pH values (<pK_a), the protonation of the fatty tertiary amine in piperazine part of the probe restrains the electron transfer from the amino to the fluorophore, which results in high fluorescence. When the sample becomes more basic, the protonated piperazine is deprotonated, and the electron transfer from the amino to the fluorophore is restored again, which leads to a decrease in the fluorescence intensity. Saccharide binding increases the acidity of phenylboronic acid producing a more electron deficient boron atomic centre. Therefore, a stronger interaction between boronic acid and amine could be expected upon saccharide binding, which depresses the electron transfer process and leads to a higher fluorescence (Scheme 2). The slight red shifts in the absorption and emission maxima could be attributed to the deprotonation of the protonated piperazine strengthening the electron push–pull effect of the probe to some extent.

Spectral responses of both probes toward sugars

Next, we explored the effects of sugars on the absorption and emission spectra of both probes. Fig. 4 demonstrates that with increasing D-fructose concentration the absorbance of both probes increase accompanied with clear blue shifts in absorption maxima (from 400 nm to 392 nm). Significant fluorescence enhancements of both probed are observed upon the addition of D-fructose. The introduction of 100 mM D-fructose induces about 50-fold and 5-fold fluorescence enhancements for **PET-S1** and **PET-S2**, respectively. But D-fructose causes the emission bands of **PET-S1** and **PET-S2** shift to different directions (Fig. 4 and S4†): ~10 nm blue-shift for **PET-S1** (from 540 nm to

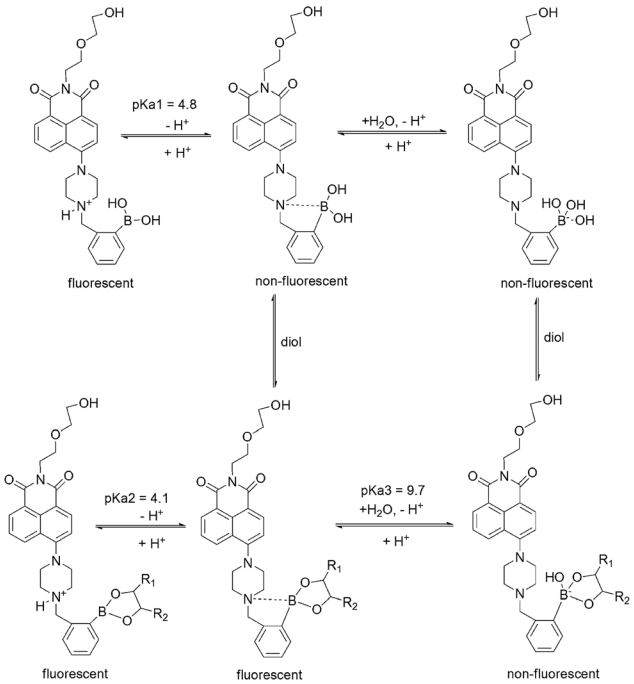

Scheme 2 Complexation of sugars with **PET-S1** in water.

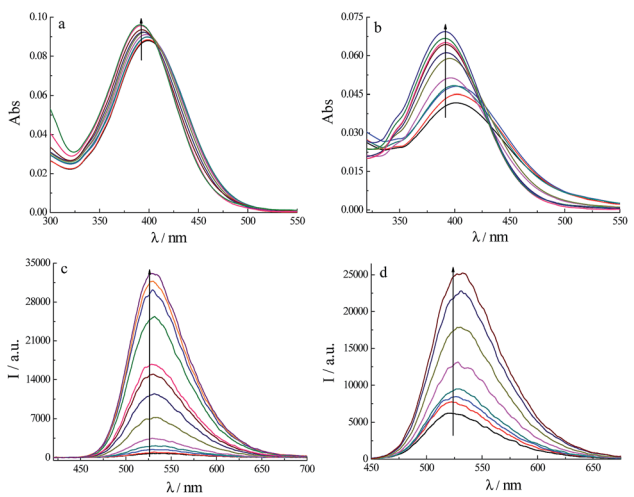

Fig. 4 UV-vis (a and b) and fluorescence (c and d) spectral changes of **PET-S1** (a and c) and **PET-S2** (b and d) in the presence of different concentrations of D-fructose. [**PET-S1**] = [**PET-S2**] = 10 μM, [D-fructose] = 0–300 mM, 50 mM PBS, pH 7.4, λ_{ex} = 400 nm. Each spectrum was recorded 1 min after the addition of the sugar.

530 nm), while ~9 nm red-shift for **PET-S2** (from 521 nm to 530 nm). The blue-shift caused by sugar may be due to the tighter interaction of B–N bonding creating a weaker electron-donating fatty amino. The red-shift in the fluorescence spectrum of **PET-S2** could be ascribed to dis-association of H-aggregates of **PET-S2** upon sugar binding.[3h] D-Fructose triggered much higher fluorescence enhancement of **PET-S1** than that of **FR-530**,[4a] implying that the rigid piperazine benefits the formation of B–N bonding. The higher fluorescence of both compounds in more viscous media supports the above hypothesis (Fig. S1b,† the presence of 400 mM of glycerol induced only 3-fold fluorescence enhancement, which infers that the effect of the dihydric alcohol on the fluorescence intensity of the probe is very small).

Other sugars such as D-sorbitol, D-galactose, D-glucose and D-mannose induced similar spectral changes but to different degrees (Fig. 5). The fluorescence quantum yields of both probes in the absence and presence of the sugars were summarized in Table 1. The results suggest that **PET-S1** has some advantages over **PET-S2**: more sensitive and better solubility. Therefore, **PET-S1** was employed as the probe in detection of D-fructose in the realistic samples. It is interesting to note that glucose, mannose and galactose did not trigger obvious spectral change of **PEI-S2** (Fig. S5†), which reveals that **PET-S2** has good selecivity toward fructose and sorbitol.

Fig. 5 shows the fluorescence intensity of **PET-S1** *vs.* sugar concentration. It is clear that **PET-S1** is much more sensitive to fructose and sorbitol than to other three sugars. To further study the binding interaction between the probes and sugars, association constants have been estimated using the following equation.[12]

$$(I_{max} - I_0)/(I_c - I_0) = 1 + (Kc)^{-1} \quad (1)$$

where I_0, I_c and I_{max} are the fluorescence intensities of the probe alone, in the presence of c mol L^{-1} sugar and a large excess of sugar, respectively; K is the association constant and c is the sugar concentration added. Good linear relationships between $(I_{max} - I_0)/(I_c - I_0)$ and $1/c$ for **PET-S1** were obtained (Fig. 6), the binding constant K values were determined and listed in Table 2. The binding constants between **PET-S1** and sugars decrease in the following order: D-sorbitol > D-fructose > D-galactose > D-mannose > D-glucose, which is consistent with the published results.[3g,4a,8b,c] The effect of biglycan sucrose was negligible as sucrose concentration less than 30 mM (Fig. S6†).

The detection limit (LOD) was obtained by $3S_b/k$, where S_b is the standard deviation of the blank measurements of 10 times, and k is the slope of the fitted line (Fig. S7†). The lower detection limits of fructose and sorbitol are corresponding to their higher binding abilities toward **PET-S1** (Table 2).

The detection of fructose in drinks

Considering the high selecivity and competition of **PET-S1** toward D-fructose over some other sugars (Fig. S8†) probably existing in drinks and high fructose contents in honey and some beverages, finally, we employed **PET-S1** to detect fructose in honey and some beverages. Table 3 indicates that **PET-S1** is able to determine the concentrations of spiked D-fructose in honey and beverages with good recovery, revealing that this probe can potentially be used for quantitatively detecting D-fructose in realistic samples.

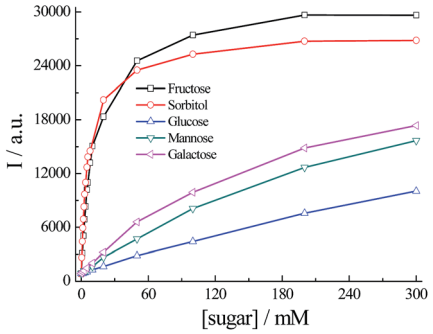

Fig. 5 The fluorescence intensity changes of **PET-S1** as a function of sugar concentration. [**PET-S1**] = 10 μM, 50 mM PBS, pH 7.4.

Table 1 The fluorescence quantum yields of both probes in the absence and presence of sugars

Sugar	None	Fructose	Sorbitol	Glucose	Mannose	Galactose
Φ_f[a]						
PET-S1	0.007	0.222	0.189	0.066	0.085	0.077
FE[b]	—	32.3	27.4	9.6	12.3	11.2
PET-S2	0.065	0.213	0.207	0.080	0.088	0.057
FE[b]	—	3.3	3.2	1.2	1.4	0.9

[a] Coumarin 153 (Φ = 0.38 in ethanol) was used as the reference, [**PET-S1**] = [**PET-S2**] = 10 μM, [sugar] = 300 mM, 50 mM PBS, pH 7.4. [b] Fluorescent enhancement (FE) is the ratio of quantum yield with sugar and that without sugar.

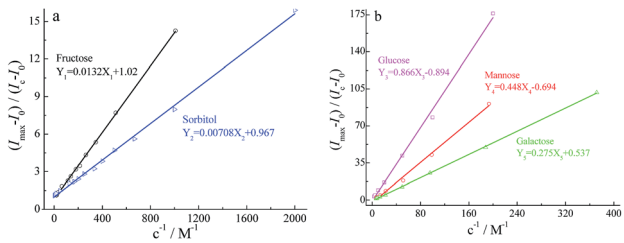

Fig. 6 Plots of $(I_{max} - I_0)/(I_c - I_0)$ against c^{-1} for **PET-S1** with different sugars. [**PET-S1**] = 10 μM, 50 mM PBS, pH 7.4.

Table 2 The association constants (K_{as}) between **PET-S1** and different sugars and their detection limits (LOD)

	Fructose	Sorbitol	Glucose	Mannose	Galactose
K_{as}/M^{-1}	75.8	140.8	1.2	2.2	3.6
LOD/mM	0.045	0.028	2.62	1.14	0.72

Table 3 Determination of D-fructose concentrations in beverages

Sample	Fructose added/mM	Fructose found/mM	Recovery%	RSD[a]%
Kangshifu sugar Sydney[b]	0	1.63		2.6
	1.0	2.83	120	2.8
	2.0	3.92	115	1.4
	3.0	4.75	104	2.1
Kangshifu honey grapefruit[b]	0	1.61		2.2
	1.0	2.78	117	2.9
	2.0	3.83	111	0.3
	3.0	4.42	93.3	1.4
Milk vetch honey[c]	0	2.05		3.1
	1.0	3.04	99.0	2.1
	2.0	3.74	84.5	2.6
	3.0	4.65	86.7	1.2

[a] Relative standard derivations were calculated on the basis of three measurements. [b] 150 folds diluted with PBS and. [c] 1.80 g of honey dissolved in 3000 mL PBS.

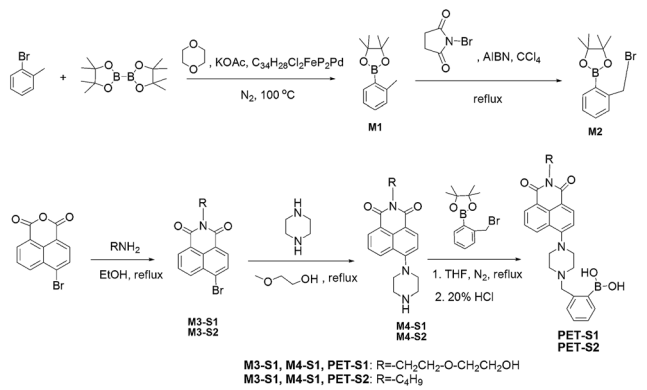

Scheme 3 The synthesis procedures of PET-S1 and PET-S2.

Conclusions

Two fluorescent sensors were developed for sensitive detection of saccharides in aqueous solution based on the photoinduced electron transfer. The presence of rigid piperazine strengthens the interaction between the boronic acid and the amino, and much higher fluorescence enhancements are obtained upon saccharides binding. Probe **PET-S1** has good water-solubility and large Stokes shift (~130 nm), which ensures it a potential sensor for sugars in realistic samples. This work may inspire the design of new fluorescence probes for sensitive recognition of sugars.

Experimental

Synthesis

PET-S1 and **PET-S2** were synthesized according to the following procedures (Scheme 3).

M1. 2-Bromotoluene (2.00 g, 11.77 mmol), bis(pinacolato) diboron (3.27 g, 12.86 mmol), potassium acetate (3.44 g, 35.05 mmol) and [1,1′-bis(diphenylphosphino)ferrocene] dichloropalladium(II) (85.56 mg, 0.12 mmol) were added into 55 mL dioxane. The mixture was stirred at ~100 °C under N_2 atmosphere for 18 h. The reaction progress was traced by TLC. After cooling to room temperature, the reaction solution was mixed with 55 mL ethyl acetate and then filtered to separate the solid. The filter liquor was washed with brine and dried over anhydrous $MgSO_4$. The organic layer was concentrated under vacuum pump and purified by column chromatography [petroleum ether : ethyl acetate = 100 : 1 (V : V)] to give **M1** as light yellow oil (1.55 g, 60.7%). ^{1}H-NMR (400 MHz, $CDCl_3$) δ (ppm): 7.76 (d, J = 6.5 Hz, 1H), 7.31 (t, J = 6.1 Hz, 1H), 7.19–7.12 (m, 2H), 2.54 (s, 3H), 1.33 (s, 12H).

M2. Compound **M1** (1.50 g, 6.88 mmol) was dissolved in 40 mL CCl_4 and heated to refluxing. Then *N*-bromosuccinimide (NBS, 1.71 g, 9.66 mmol) and azodiisobutyronitrile (AIBN, 101.64 mg, 0.62 mmol) were added into the above solution. After refluxing for 30 h, the solvent was removed under reduced pressure to afford crude product, which was purified by column chromatography [petroleum ether : ethyl acetate = 200 : 1 (V : V)] to yield **M2** as white crystals (1.24 g, 60.8%). ^{1}H-NMR (400 MHz, $CDCl_3$) δ (ppm): 7.74 (d, J = 7.2 Hz, 1H), 7.35–7.27 (m, 2H), 7.23–7.17 (m, 1H), 4.83 (s, 2H), 1.28 (s, 12H).

M3-S1 and **M3-S2** were synthesized according to the ref. 13 **M3-S1** (78.3%). ^{1}H-NMR (400 MHz, $CDCl_3$) δ (ppm): 8.67 (d, J = 7.3 Hz, 1H), 8.59 (d, J = 8.5 Hz, 1H), 8.43 (d, J = 7.9 Hz, 1H), 8.05 (d, J = 7.9 Hz, 1H), 7.86 (dd, J = 7.5, 8.3 Hz, 1H), 4.45 (q, J = 5.6 Hz, 2H), 3.86 (q, J = 5.6 Hz, 2H), 3.72–3.64 (m, 4H), 2.43 (t, J = 5.6 Hz, 1H). **M3-S2** (92.0%) ^{1}H-NMR (400 MHz, $CDCl_3$) δ (ppm): 8.65 (d, J = 7.3 Hz, 1H), 8.56 (d, J = 8.5 Hz, 1H), 8.41 (d, J = 7.9 Hz, 1H), 8.04 (d, J = 7.9 Hz, 1H), 7.85 (dd, J = 7.4, 8.4 Hz, 1H), 4.17 (q, J = 7.5 Hz, 2H), 1.76–1.67 (m, 2H), 1.50–1.40 (m, 2H), 0.98 (q, J = 7.3 Hz, 3H).

The synthesis of M4-S1. 1.55 g **M3-S1** (4.26 mmol) and 440 mg piperazine (5.11 mmol) were added into 200 mL 2-methoxyethanol. The reaction solution was refluxed and traced by TLC. After the raw material exhausted, the solvent was removed under reduced pressure to afford crude product, which was purified by column chromatography [CH_2Cl_2 : CH_3OH = 80 : 1–10 : 1 (V : V)] to afford **M4-S1** as yellow solid (1.1 g, 67.0%). ^{1}H-NMR

(400 MHz, DMSO-d_6) δ (ppm): 8.47 (dd, J = 6.0, 8.4 Hz, 2H), 8.40 (d, J = 8.1 Hz, 1H), 7.81 (t, J = 8.2 Hz, 1H), 7.33 (d, J = 8.2 Hz, 1H), 4.59 (bar, 1H), 4.23 (t, J = 6.6 Hz, 2H), 3.64 (t, J = 6.5 Hz, 2H), 3.46 (bar, 4H), 3.22–3.16 (m, 4H), 3.07 (t, J = 4.5 Hz, 4H).

M4-S2 was obtained by the same procedure with **M3-S2** instead of **M3-S1** (71.5%). ^{1}H-NMR (400 MHz, DMSO-d_6) δ (ppm): 8.47 (dd, J = 2.6, 7.2 Hz, 2H), 8.40 (d, J = 8.1 Hz, 1H), 7.81 (t, J = 7.4 Hz, 1H), 7.34 (d, J = 8.1 Hz, 1H), 4.03 (t, J = 7.3 Hz, 2H), 3.20 (t, J = 4.7 Hz, 4H), 3.10 (t, J = 4.7 Hz, 4H), 1.64–1.54 (m, 2H), 1.39–1.28 (m, 2H), 0.92 (t, J = 7.3 Hz, 3H).

Synthesis of PET-S1 and PET-S2. 175 mg of **M4-S1** (0.47 mmol) and 189 mg of compound **M2** (0.64 mmol) were added into 40 mL mixed solution of THF–CH_3OH (V : V = 1 : 1). The above solution was heated to reflux under N_2 atmosphere. Then 2 mL of triethylamine was added dropwise to the above solution. After the raw material exhausted, the solvent was removed under reduced pressure to afford crude product, which was purified by column chromatography [CH_2Cl_2 : CH_3OH = 200 : 1–4 : 1 (V : V) containing 1% triethylamine] to give yellow oil. Then 20% HCl was added into the oil and the mixed solution was stirred overnight under room temperature. The resulted solution was poured into 100 mL deionized water and its pH was adjusted to ~7 with NaOH to yield yellow precipitation. The solution was filtered to obtain probe **PET-S1** as yellow solid (47 mg, 20.0%). ^{1}H-NMR (400 MHz, DMSO-d_6) δ (ppm): 9.08 (s, 2H), 8.46 (t, J = 7.7 Hz, 2H), 8.39 (d, J = 8.1 Hz, 1H), 7.81 (t, J = 7.7 Hz, 1H), 7.69 (d, J = 6.7 Hz, 1H), 7.35 (d, J = 7.9 Hz, 1H), 7.29 (t, J = 6.3 Hz, 2H), 7.25–7.19 (m, 1H), 4.66–4.60 (m, 1H), 4.22 (t, J = 6.4 Hz, 2H), 3.73 (s, 2H), 3.63 (t, J = 6.5 Hz, 2H), 3.46 (t, J = 4.6 Hz, 4H), 3.26 (bar, 4H), 2.77 (bar, 4H). ^{13}C-NMR (400 MHz, DMSO-d_6): 163.55, 163.01, 155.33, 141.07, 135.02, 132.21, 130.71, 130.54, 129.92, 129.13, 129.08, 126.84, 126.15, 125.28, 122.47, 115.67, 115.17, 72.05, 66.90, 62.77, 60.11, 52.07, 51.59, 38.56. HR-MS observed m/z: 504.2306 $(M + H)^+$, 518.2462 $(M + CH_3)^+$; calculated molecular weight of $C_{27}H_{31}BN_3O_6$: 504.2306 for $(M + H)^+$, $C_{28}H_{33}BN_3O_6$: 518.2462 for $(M + CH_3)^+$.

PET-S2 was obtained by the same procedure with **M4-S2** instead of **M4-S1** (35.0%). ^{1}H-NMR (400 MHz, $CDCl_3$) δ (ppm): 8.93 (bar, 2H), 8.58 (d, J = 7.2 Hz, 1H), 8.50 (d, J = 8.0 Hz, 1H), 8.37 (d, J = 8.4 Hz, 1H), 7.98 (d, J = 8.5 Hz, 1H), 7.69 (t, J = 7.5 Hz, 1H), 7.42–7.35 (m, 2H), 7.26–7.20 (m, 2H), 4.16 (t, J = 7.5 Hz, 2H), 3.81 (s, 2H), 3.31 (bar, 4H), 2.88 (bar, 4H), 1.75–1.66 (m, 2H), 1.50–1.38 (m, 2H), 0.97 (t, J = 7.3 Hz, 3H). ^{13}C-NMR (400 MHz, $CDCl_3$): 164.42, 163.96, 155.14, 140.32, 136.54, 132.43, 131.14, 130.78, 130.33, 129.84, 129.78, 127.80, 126.19, 125.90, 123.38, 117.37, 115.28, 52.42, 52.07, 64.20, 40.12, 30.24, 20.39, 13.86. HR-MS observed m/z: 472.2409 $(M + H)^+$, calculated molecular weight of $C_{27}H_{31}BN_3O_4$: 472.2408 for $(M + H)^+$.

Acknowledgements

This work was financially supported by National 973 Program (no. 2011CB910403), NSFC (no. 21235005) and Shanghai Municipal Natural Science Foundation. We thank Dr H.-Y. Tian (East China University of Science & Technology) for his kind help.

Notes and references

1 (*a*) K. A. Wintergerst, B. Buckingham, L. Gandrud, B. J. Wong, S. Kache and D. M. Wilson, *Pediatrics*, 2006, **118**, 173; (*b*) S. Finfer, B. Liu, D. R. Chittock, R. Norton, J. A. Myburgh, C. McArthur, I. Mitchell, D. Foster, V. Dhingra, W. R. Henderson, J. J. Ronco, R. Bellomo, D. Cook, E. McDonald, P. Dodek, P. C. Hébert, D. K. Heyland and B. G. Robinson, *N. Engl. J. Med.*, 2012, **367**, 1108; (*c*) M. J. Gillett, *Clin. Biochem. Rev.*, 2009, **30**, 197; (*d*) N. Bouteldja and D. J. Timson, *J. Inherited Metab. Dis.*, 2010, **33**, 105; (*e*) M. I. Yasawy, U. R. Folsch, W. E. Schmidt and M. Schwend, *World J. Gastroenterol.*, 2009, **15**, 2412.

2 (*a*) J. S. Kim and D. T. Quang, *Chem. Rev.*, 2007, **107**, 3780; (*b*) T. Q. Duong and J. S. Kim, *Chem. Rev.*, 2010, **110**, 6280; (*c*) M. S. T. Gonçalves, *Chem. Rev.*, 2009, **109**, 190; (*d*) Q. Sun, J. Qian, H. Tian, L. Duan and W. Zhang, *Chem. Commun.*, 2014, **50**, 8518; (*e*) H. S. Jung, X. Chen, J. S. Kim and J. Yoon, *Chem. Soc. Rev.*, 2013, **42**, 6019.

3 For some examples: (*a*) Z. Guo, I. Shin and J. Yoon, *Chem. Commun.*, 2012, **48**, 5956; (*b*) H. S. Mader and O. S. Wolfbeis, *Microchim. Acta*, 2008, **162**, 1; (*c*) X. Yang, C. Dai, A. Dayan, C. Molina and B. Wang, *Chem. Commun.*, 2010, **46**, 1073; (*d*) X. Wu, Z. Li, X.-X. Chen, J. S. Fossey, T. D. James and Y.-B. Jiang, *Chem. Soc. Rev.*, 2013, **42**, 8032; (*e*) S. Akay, W. Yang, J. Wang, L. Lin and B. Wang, *Chem. Biol. Drug Des.*, 2007, **70**, 279; (*f*) S. Saito, T. L. Massie, T. Maeda, H. Nakazumi and C. L. Colyer, *Sensors*, 2012, **12**, 5420; (*g*) S. Jin, J. F. Wang, M. Y. Li and B. H. Wang, *Chem.–Eur. J.*, 2008, **14**, 2795; (*h*) H. Bai, Q. Sun, H. Tian, J. Qian, L. Zhang and W. Zhang, *Chin. J. Chem.*, 2013, **31**, 1095.

4 (*a*) S. Trupp, A. Schweitzer and G. J. Mohr, *Org. Biomol. Chem.*, 2006, **4**, 2965; (*b*) Z. Xing, H. Wang, Y. Cheng, C. Zhu, T. D. James and J. Zhao, *Eur. J. Org. Chem.*, 2012, 1223; (*c*) T. D. James, K. R. A. S. Sandanayake and S. Shinkai, *Angew. Chem., Int. Ed. Engl.*, 1994, **33**, 2207; (*d*) T. D. James, K. R. A. S. Sandanayake and S. Shinkai, *J. Chem. Soc., Chem. Commun.*, 1994, 477.

5 (*a*) K. R. A. S. Sandanayake and S. Shinkai, *J. Chem. Soc., Chem. Commun.*, 1994, 1083; (*b*) X. Gao, Y. Zhang and B. Wang, *Org. Lett.*, 2003, **5**, 4615; (*c*) X. Gao, Y. Zhang and B. Wang, *New J. Chem.*, 2005, **29**, 579; (*d*) J. Yoon and A. W. Czarnik, *J. Am. Chem. Soc.*, 1992, **114**, 5874.

6 S. Arimori, M. L. Bell, C. S. Oh and T. D. James, *Org. Lett.*, 2002, **4**, 4249.

7 (*a*) L. H. Feng, F. Liang, Y. Wang and X. J. Wang, *Sens. Actuators, B*, 2012, **173**, 575; (*b*) Z. J. Wang, H. Y. Lei, C. Y. Zhou, G. F. Wang and L. H. Feng, *Spectrochim. Acta, Part A*, 2012, **91**, 178.

8 For some examples: (*a*) Y. J. Huang, W. J. Ouyang, X. Wu, Z. Li, J. S. Fossey, T. D. James and Y. B. Jiang, *J. Am. Chem. Soc.*, 2013, **135**, 1700; (*b*) J. Zhai, T. Pan, J. Zhu, J. Xu,

J. Chen, Y. Xie and Y. Qin, *Anal. Chem.*, 2012, **84**, 10214; (*c*) Y. Cheng, N. Ni, W. Yang and B. Wang, *Chem.–Eur. J.*, 2010, **16**, 13528; (*d*) K. Guzow, D. Jażdżewska and W. Wiczk, *Tetrahedron*, 2012, **68**, 9240; (*e*) W. Yang, L. Lin and B. Wang, *Tetrahedron Lett.*, 2005, **46**, 7981; (*f*) X. Gao, T. McGill and M. D. Heagy, *J. Org. Chem.*, 2004, **69**, 2959; (*g*) Y.-P. Li, L. Jiang, T. Zhang, M. Lin, D.-B. Tian and H. Huang, *Chin. Chem. Lett.*, 2014, **25**, 77.

9 (*a*) M. E. Jun, B. Roy and K. H. Ahn, *Chem. Commun.*, 2011, **47**, 7583; (*b*) Q.-C. Xu, X.-H. Zhu, C. Jin, G.-W. Xing and Y. Zhang, *RSC Adv.*, 2014, **4**, 3591; (*c*) L. E. Santos-Figueroa, M. E. Moragues, E. Climent, A. Agostini, R. Martínez-Máñez and F. Sancenón, *Chem. Soc. Rev.*, 2013, **42**, 3489; (*d*) H. Li, J. Fan and X. Peng, *Chem. Soc. Rev.*, 2013, **42**, 7943.

10 A. P. de Silva, H. Q. N. Gunaratne, T. Gunnlaugsson, A. J. M. Huxley, C. P. McCoy, J. T. Rademacher and T. E. Rice, *Chem. Rev.*, 1997, **97**, 1515.

11 (*a*) J. Ren, Z. Wu, Y. Zhou, Y. Li and Z. Xu, *Dyes Pigm.*, 2011, **91**, 442; (*b*) M. H. Lee, J. H. Han, J.-H. Lee, H. G. Choi, C. Kang and J. S. Kim, *J. Am. Chem. Soc.*, 2012, **134**, 17314; (*c*) L. Zhang, D. Duan, Y. Liu, C. Ge, X. Cui, J. Sun and J. Fang, *J. Am. Chem. Soc.*, 2014, **136**, 226; (*d*) C. Huang, Q. Yin, W. Zhu, Y. Yang, X. Wang, X. Qian and Y. Xu, *Angew. Chem., Int. Ed.*, 2011, **50**, 7551; (*e*) L. Song, T. Jia, W. Lu, N. Jia, W. Zhang and J. Qian, *Org. Biomol. Chem.*, 2014, **12**, 8422.

12 (*a*) S. A. Moore, K. M. Glenn and R. M. Palepu, *J. Solution Chem.*, 2007, **36**, 563; (*b*) B. K. Paul, A. Samanta and N. Guchhait, *J. Phys. Chem. B*, 2010, **114**, 6183.

13 (*a*) H. Tian, J. Qian, H. Bai, Q. Sun, L. Zhang and W. Zhang, *Anal. Chim. Acta*, 2013, **768**, 136; (*b*) J. Qian, X. Qian, Y. Xu and S. Zhang, *Chem. Commun.*, 2008, 4141; (*c*) J. Qian, Y. Xu, X. Qian, J. Wang and S. Zhang, *J. Photochem. Photobiol., A*, 2008, **200**, 402.